Hindawi Publishing Corporation
EURASIP Journal on Advances in Signal Processing
Volume 2011, Article ID 507215, 9 pages
doi:10.1155/2011/507215

Research Article

An Improved Flowchart for Gabor Order Tracking with Gaussian Window as the Analysis Window

Yang Jin[1,2] and Zhiyong Hao[1]

[1] *Department of Energy Engineering, Power Machinery and Vehicular Engineering Institute, Zhejiang University, Hangzhou 310027, China*
[2] *Department of Automotive Engineering, Hubei University of Automotive Technology, Shiyan 442002, China*

Correspondence should be addressed to Yang Jin, jin_yang@163.com

Received 1 July 2010; Revised 21 November 2010; Accepted 19 December 2010

Academic Editor: Antonio Napolitano

Based on simulations on the ability of the Gaussian-function windowed Gabor coefficient spectrum to separate order components, an improved flowchart for Gabor order tracking (GOT) is put forward. With a conventional GOT flowchart with Gaussian window, successful order waveform reconstruction depends significantly on analysis parameters such as time sampling step, frequency sampling step, and window length in point number. A trial-and-error method is needed to find such parameters. However, an automatic search with an improved flowchart is possible if the speed-time curve and order difference between adjacent order components are known. The appropriate analysis parameters for a successful waveform reconstruction of all order components within a given order range and a speed range can be determined.

1. Introduction

Because of the inherent mechanism features, the frequency contents of the main excitations in rotary machinery are integer or fractional multiples of a fundamental frequency, which is usually the rotary speed of the machine [1]. The integer or fractional multiples of the fundamental frequency are called "harmonics" or "orders." A machine's run-up or run-down operation is a typical nonstationary process. The excitations in the machine are analogous to frequency-sweep excitations with several excitation frequencies at a time instant because the fundamental frequency is time varying. The vibroacoustic signals acquired during this stage carry information about structural dynamics. Information extraction from these signals is important. Order tracking (OT) is a dedicated nonstationary signal processing technique dealing with rotary machinery. Several computational OT techniques have been developed, such as resampling OT [1], Vold-Kalman OT [2, 3], and Gabor OT (GOT) [4], each with its strengths and shortcomings. Among them, GOT can easily implement the reconstruction of order waveforms, but it has the following limitations.

(i) It is not suitable for signals with cross-order components [5].
(ii) The appropriate analysis parameters are determined by the trial-and-error method (human-computer interaction) to separate order components in the Gabor coefficient spectrum. However, no reports have explained how to find the appropriate parameters.

In this study, we addressed the second limitation, and established a flowchart for GOT without trial and error. We first generalized the conditions from simulations under which a Gabor coefficient spectrum with a Gaussian window can separate order components, and then combined the conditions and current GOT technique for an improved flowchart.

This paper is organized as follows. Section 2 introduces the GOT and the convergence conditions for the reconstructed order waveform. Section 3 investigates the ability of a Gabor coefficient spectrum with Gaussian window to separate order components using simulation. Section 4 explains the improved flowchart. Section 5 verifies the proposed flowchart. Section 6 concludes the paper.

2. GOT and the Convergence Conditions for the Reconstructed Order Waveforms

2.1. Discrete Gabor Transform and Gabor Expansion. GOT is based on the transform pair of discrete Gabor transform (1) and Gabor expansion (2) [6]. Gabor expansion is also called Gabor reconstruction or synthesis:

$$\begin{aligned}\widetilde{c}_{m,n} &= \sum_{i=m\Delta M-L/2}^{m\Delta M+L/2-1} s[i]\gamma^*_{m,n}[i], \\ &= \sum_{i=m\Delta M-L/2}^{m\Delta M+L/2-1} s[i]\gamma^*[i-m\Delta M]e^{-j2\pi ni/N},\end{aligned} \tag{1}$$

$$\begin{aligned}s[i] &= \sum_{m=0}^{M-1}\sum_{n=0}^{N-1} \widetilde{c}_{m,n}h_{m,n}[i] \\ &= \sum_{m=0}^{M-1}\sum_{n=0}^{N-1} \widetilde{c}_{m,n}h[i-m\Delta M]e^{j2\pi ni/N},\end{aligned} \tag{2}$$

where $s[i]$ is the signal, $i, m, n, \Delta M, M, N, L \in Z$, ΔM denotes the time sampling step in the point number; M denotes the time sampling number, N denotes the frequency sampling number or frequency bins; and L denotes the window length in point number, and "$*$" denotes complex conjugate operation.

The set of the functions $\{h_{m,n}[i]\}_{m,n\in Z}$ is the Gabor elementary functions, also termed as the set of synthetic functions, and $\{\gamma_{m,n}[i]\}_{m,n\in Z}$ is the set of analysis functions. $h[i]$ is the synthetic window and $\gamma[i]$ is the analysis window. Thus, $\{h_{m,n}[i]\}_{m,n\in Z}$ and $\{\gamma_{m,n}[i]\}_{m,n\in Z}$ are the time-shifted and harmonically modulated versions of $h[i]$ and $\gamma[i]$, respectively.

Equation (1) shows that the Gabor coefficients, $\widetilde{c}_{m,n}$, are the sampled short-time Fourier transform with the window function $\gamma[i]$. To utilize the FFT, the frequency bin, N, is set to be equal to L, which has to be a power of 2. L has to be divided by both N and ΔM in view of numerical implementation. For stable reconstruction, the oversampling rate defined by

$$r_{\text{os}} = \frac{N}{\Delta M} \tag{3}$$

must be greater or equal to one. It is called the critical sampling rate when γ_{os} equals one. The critical sampling means the number of Gabor coefficients is equal to the number of signal samples.

Equation (2) exists if and only if $h[i]$ and $\gamma[i]$ form a pair of dual functions [7]. Their positions in (1) and (2) are interchangeable.

2.2. Convergence Conditions for Reconstructed Order Waveforms. Given $h[i]$, ΔM and N, generally, the solution of $\gamma[i]$ is not unique. If viewed only from pure mathematics, we can perfectly reconstruct the signal $s[i]$ with (1) and (2) as long as $\gamma_{\text{os}} \geq 1$ and $\gamma[i]$ is a dual function of $h[i]$, regardless whether $h[i]$ and $\gamma[i]$ are like. However, the idea behind GOT is to reconstruct the different order components (or harmonics) in the signal. There are three other conditions for the convergence of the reconstructed order waveforms.

(i) The analysis window $\gamma[i]$ has to be localized in the joint time-frequency domain so that $\widetilde{c}_{m,n}$ will depict the signal's time-frequency properties. In the context of rotary machinery, $\widetilde{c}_{m,n}$ are desired to describe the signal's time-varying harmonics for a run-up or run-down signals.

(ii) The time-frequency resolution of $\gamma[i]$ should be able to separate adjacent harmonics within the desired order range and rotary speed range.

(iii) The behaviors of $h[i]$ and $\gamma[i]$, such as time/frequency centers and time/frequency resolution, have to be close. Only in this way will the reconstructed time waveform with (4) converge to the actual order component:

$$\begin{aligned}&\hat{s}_p[i] \\ &= \sum_{m=0}^{M-1}\sum_{n=0}^{N-1} \hat{c}_{m,n}h_{m,n}[i] = \sum_{m=0}^{M-1}\sum_{n=0}^{N-1} \hat{c}_{m,n}h[i-m\Delta M]e^{j2\pi ni/N},\end{aligned} \tag{4}$$

where $\hat{c}_{m,n}$ denotes the extracted Gabor coefficients associated with the desired order p, and $\hat{\text{s}}_p[i]$ denotes the reconstructed p_{th} order component waveform.

Given a window function $h[i]$, the Gabor transform's time sampling step ΔM, and the frequency sampling step N, the orthogonal-like Gabor expansion technique [8], which seeks the optimal dual window so that the dual window $\gamma[i]$ most approximates a real-value scaled $h[i]$, has been developed. When $h[i]$ is the discrete Gaussian function, that is,

$$h[i] = g[i] = \sqrt[4]{\frac{1}{2\pi(\sigma^D)^2}}e^{-1/4(i/\sigma^D)^2} \quad \forall i \in \left[-\frac{L}{2}, \frac{L}{2}-1\right], \tag{5}$$

then when

$$\left(\sigma^D\right)^2 = \left(\sigma^D_{\text{opt}}\right)^2 = \frac{\Delta M \cdot N}{4\pi}, \tag{6}$$

the obtained dual window by the orthogonal-like technique is the optimal [7]. Moreover, the optimal dual window is related to the oversampling rate. Generally, the difference between a window and its optimal dual window decreases as the oversampling rate increases. The difference between the analysis and synthesis windows is negligible for the commonly used window functions, such as the Gaussian and Hanning windows when the oversampling rate is not less than four [7]. The window in this study is limited to the Gaussian window.

2.3. Conventional Flowchart for GOT. Figure 1 is the flowchart for the conventional GOT routine. There is no

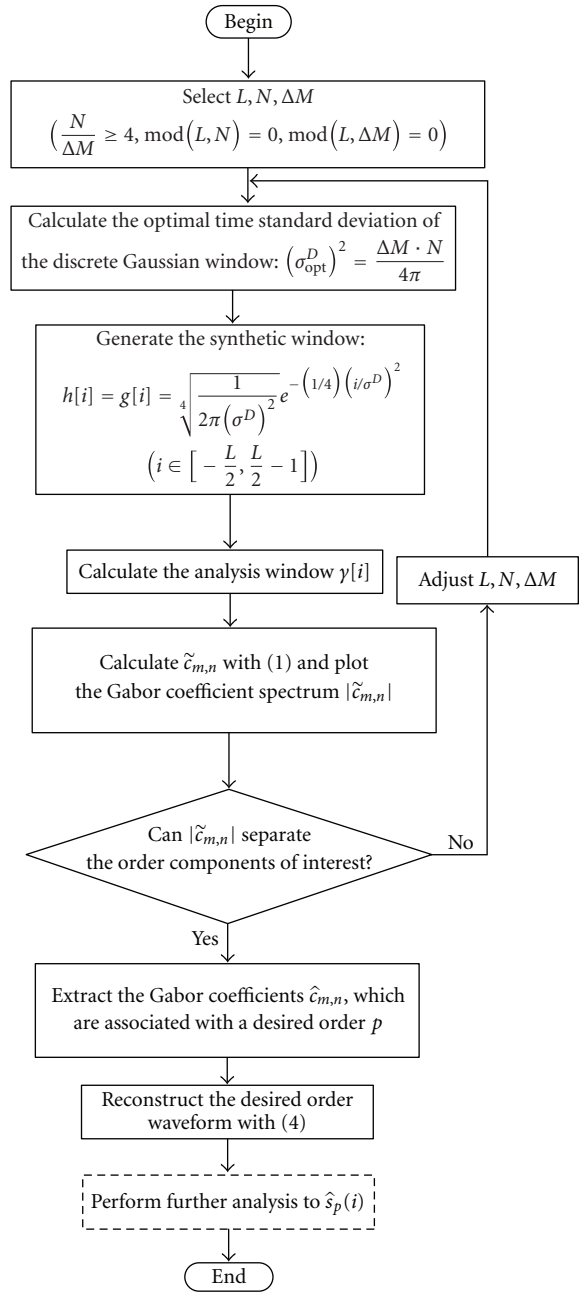

($\mathrm{mod}(x, y)$ denotes computing the remainder of x/y)

Figure 1: Flowchart for the conventional GOT.

problem about the convergence conditions (1) and (3), while condition (2) is satisfied using the trial-and-error method.

In conventional GOT flowcharts, human-computer interaction is needed to determine the appropriate analysis parameters. Each time the analysis parameters are changed, the user needs to give a visual inspection to the obtained Gabor coefficient spectrum to judge how well the order components are separated in the spectrum. If it fails, then the analysis parameters are adjusted to get another Gabor coefficient spectrum.

3. Simulation Investigation on the Ability of the Gabor Coefficient Spectrum with Gaussian Window to Separate Order Components

To examine the ability of the Gabor coefficient spectrum to separate order components quantitatively, the Gaussian window, which is optimally localized in the time-frequency domain, is used as the analysis window. The time standard deviation σ_t in seconds of the Gaussian window in the continuous time domain is utilized as an input parameter to generate the discrete window in discrete Gabor transform. Its

advantage is that it is easy to find the relationship between σ_t and the signal's characteristic because the signals of interest come originally from the continuous time domain.

3.1. The Gaussian Window and Its Time Standard Deviation. The energy-normalized discrete Gaussian window is

$$\begin{aligned} g[i] &= \sqrt[4]{\frac{1}{2\pi(\sigma^D)^2}}\, e^{-1/4(i/\sigma^D)^2} = \sqrt[4]{\frac{1}{2\pi(\sigma_t f_s)^2}}\, e^{-1/4(i/(\sigma_t f_s))^2} \\ &= \sqrt[4]{\frac{1}{2\pi(\sigma_t f_s)^2}}\, e^{-L^2/(4\sigma_t^2 f_s^2)(i/L)^2} \\ &= \sqrt[4]{\frac{1}{2\pi(\sigma_t f_s)^2}}\, e^{-1/(4\sigma_N{}^2)(i/L)^2} \qquad \forall i \in \left[-\frac{L}{2}, \frac{L}{2}-1\right], \end{aligned} \tag{7}$$

where f_s denotes sampling frequency, L denotes the window length in point number, σ^D denotes the standard deviation of the discrete window, and σ_t denotes the time standard deviation in seconds of the continuous time domain function $g(t)$, whose sampled version is g[i]:

$$\sigma_t = \frac{\sigma^D}{f_s}, \tag{8}$$

where σ_N denotes a normalized value defined by

$$\sigma_N = \frac{\sigma_t f_s}{L}. \tag{9}$$

Window length L should be large enough to make σ_N small enough. Small σ_N means the values at both ends of the Gaussian window are small, which will reduce the spectral leakage in Gabor transform. In our simulations, $\sigma_N \leq 0.1$ was generally guaranteed, which implies that the values at both ends of the Gaussian window are not larger than 0.2% of the window's peak value.

The frequency domain standard deviation in Herzs of $g(t)$ is

$$\sigma_f = \frac{1}{4\pi\sigma_t}. \tag{10}$$

3.2. Simulations. The discrete Gabor transform (1) is no more than a sampled short-time Fourier transform (STFT). The inherent limitation of STFT is that its time and frequency resolutions cannot be improved simultaneously. Our simulations did not aim to demonstrate this point but to disclose the conditions under which the Gabor coefficient spectrum can separate order components. We limited the frequency bins N equal to L.

Figure 2 depicts three Gabor coefficient spectra of the simulation signal $S1$ with different Gaussian window functions. For convenience of explanation, auxiliary points "0," "1," some auxiliary lines, and two characteristic values determined from numerical experiments, $6\sigma_f$ and $6\sigma_t$, are listed in this figure. In each spectrum, the abscissa is time in seconds and the ordinate is frequency in Hz. The color in the spectrum indicates the magnitude of the Gabor coefficients.

$S1$ consists of five order components and a Gaussian white noise with SNR equal to 50 (34 dB). The rotary speed $n = 60t$; the instantaneous amplitude of the p_{th} order component $A_p(t) = 1$; the instantaneous frequency of the p_{th} order component $f_p(t) = p \cdot t$.

The closer two components are located theoretically in the time-frequency domain, the more likely they will overlap in the Gabor coefficient spectrum and the more difficult it will be to distinguish them. The feature of run-up or run-down signals is that not only are there multiple components at the same time instant but there are also multiple components at the same frequency.

In Figure 2(a), at 6.82 s (indicated by line "0"), the frequency spacing between the adjacent order components is 6.82 Hz, equal to $6\sigma_f$. There are no obvious overlaps between the five components at times larger than 6.82 s. When the time is larger than 6.82 s, the theoretical time spacing between any adjacent two-order components at the same frequency is larger than $6\sigma_t$.

When σ_t is equal to 200 ms, $6\sigma_f$ is equal to 2.387 Hz (Figure 2(b)), and the instantaneous frequency spacing between the adjacent order components is larger than $6\sigma_f$ when the time is larger than 2.387 s. However, different from Figure 2(a), there are still overlaps in Figure 2(b) between the components when the time is larger than 2.387 s. These are due to the small time spacing between the adjacent order components at the same frequency. The overlaps exist between S_4 and S_5 below the frequency of about 24 Hz, at which the corresponding instant of S_4 is 6 s and that of S_5 is 4.8 s. The spacing is 1.2 s, equal to $6\sigma_t$. Similarly, the overlaps exist between S_4 and S_3 below the frequency of about 14.4 Hz, where the corresponding time of S_3 is 4.8 s, and that of S_4 is 3.6 s. The spacing is 1.2 s, also equal to $6\sigma_t$. We can explain Figure 2(c) in a similar manner.

To sum up, assume that $f_{\text{spaing,min}}$ (Hz) is the minimum theoretical frequency spacing between the adjacent order components at the same time instant and $t_{\text{spacing,min}}$ (s) is the minimum theoretical time spacing between the adjacent order components at the same theoretical frequency. If a Gabor coefficient spectrum with a Gaussian window of time standard width σ_t can separate the order components within a given order range and a speed range (i.e., the coefficient at any time-frequency sampling point is significantly the contribution from an individual component but not a combined contribution of several adjacent components), then there are the following approximate relationships:

$$f_{\text{spacing,min}} \geq 6\sigma_f = \frac{6}{4\pi\sigma_t} \Longleftrightarrow \sigma_t \geq \sigma_{t,\text{min}} = \frac{6}{4\pi f_{\text{spacing,min}}}, \tag{11}$$

$$t_{\text{spacing,min}} \geq 6\sigma_t \Longleftrightarrow \sigma_t \leq \sigma_{t,\text{max}} = \frac{t_{\text{spacing,min}}}{6}. \tag{12}$$

Inequalities (11) and (12) are the conditions for the minimum frequency spacing and the minimum time spacing, respectively.

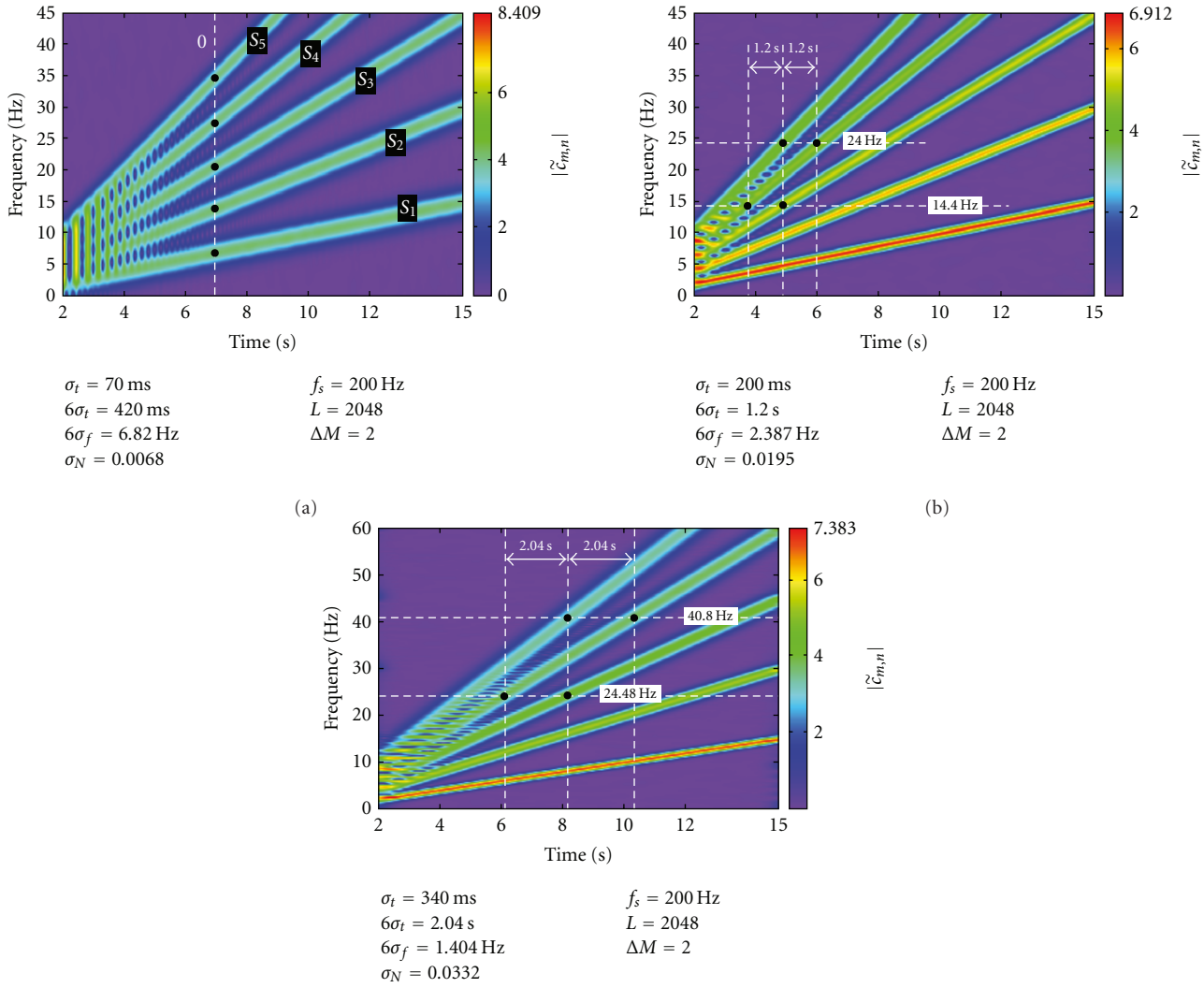

FIGURE 2: Gabor coefficient spectra with different Gaussian window widths for Signal $S1$, $S1(t) = \sum_{p=1}^{5} S_p(t) + \text{Noise}|_{\text{SNR}=50(34\,\text{dB})} = \sum_{p=1}^{5} \cos(2\pi p(t^2/2)) + \text{Noise}|_{\text{SNR}=50(34\,\text{dB})}$.

4. Improved GOT Flowchart

A Gabor coefficient spectrum that could separate the order components is obtained by trial and error in the conventional GOT flowchart. The conditions for σ_t ((11) and (12)) to separate components in the Gabor coefficient spectrum are used to improve the GOT flowchart (Figure 3). Determining $f_{\text{spaing,min}}$ and $t_{\text{spacing,min}}$ becomes the first step in the improved flowchart, and σ_t is then determined by (11) and (12) to generate the Gaussian window (analysis window). It is possible that there is no value for σ_t that could separate all order components within a given order and a speed range.

4.1. Determination of $f_{\text{spacing,min}}$ and $t_{\text{spacing,min}}$. Given a Gaussian window's σ_t for discrete Gabor transform, when the order difference between the adjacent order components are the same (Figure 4), it is liable to destroy the condition for the minimum frequency spacing with a small rotary speed. The smaller the rotary speed and the larger the order, the smaller the time spacing between adjacent order components at the same frequency and the more liable the destruction of the condition for the minimum time spacing. It can be determined from Figure 4 that

$$t_{\text{spaing,min}} = t_B = \frac{n_{\min} \cdot \Delta p}{p_{\max} \cdot k}, \tag{13}$$

$$f_{\text{spacing,min}} = \frac{n_{\min} \cdot \Delta p}{60}. \tag{14}$$

Equtions (13) and (14) hold when the speed is linearly varying and the order difference between the adjacent order components is the same. When the speed does not change this way, it is still easy to determine $f_{\text{spacing,min}}$ analytically. $f_{\text{spacing,min}} = (n_{\min}/60)\Delta p_{\min}$, where $\Delta p_{\min}$ denotes the minimum order difference between the adjacent order components. However, it would be difficult to determine

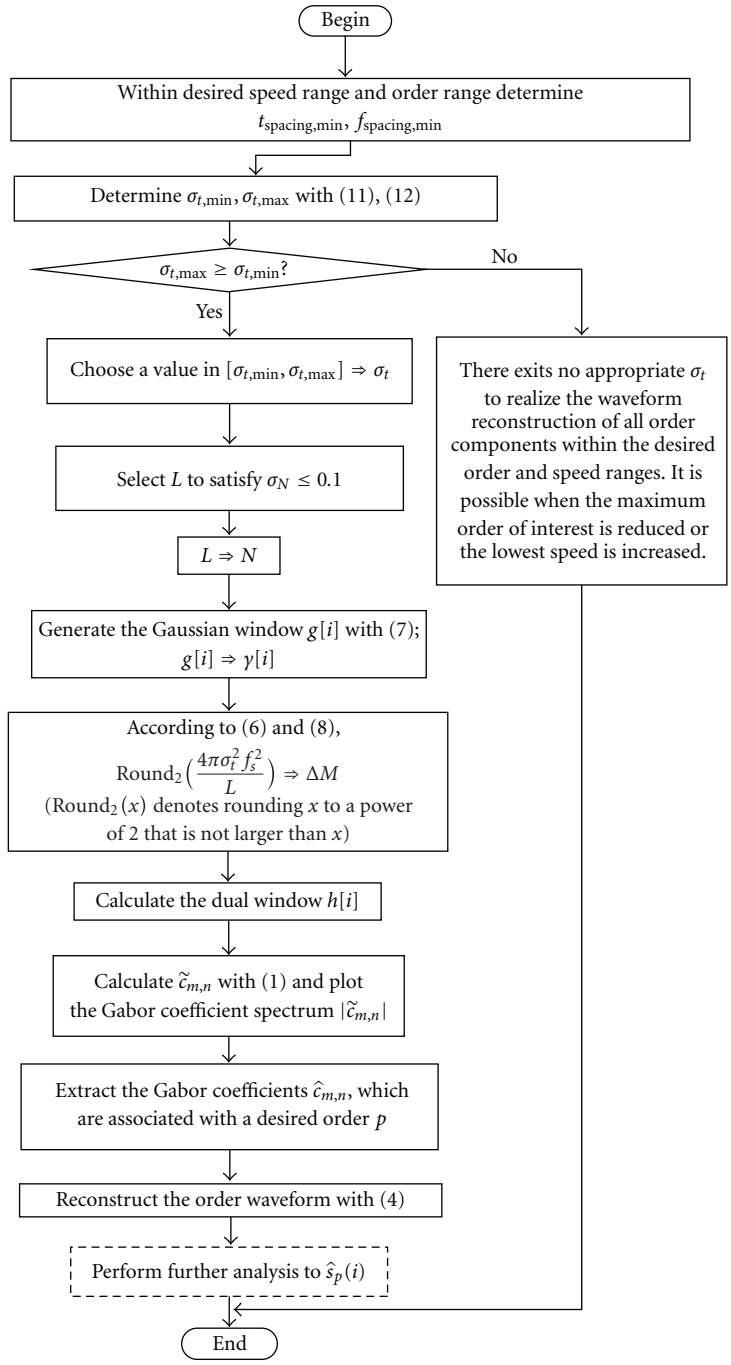

Figure 3: Flowchart for the improved GOT.

$t_{\text{spacing,min}}$ analytically even if it is not impossible. However, as long as the speed $n(t)$ changes monotonously, we can numerically determine $t_{\text{spacing,min}}$ within the given speed range $[n_{\min}, n_{\max}]$, order range $[p_{\min}, p_{\max}]$, and frequency range $[f_{\min}, f_{\max}]$. The process is described as follows (Figure 5):

(i) input $n(t)$, $[n_{\min}, n_{\max}]$, $[p_{\min}, p_{\max}]$, $[f_{\min}, f_{\max}]$, δf,

(ii) calculate the theoretical frequency curve

$$f_j(t), \quad j = 0, 1, \ldots J, \tag{15}$$

of all order components according to the speed-time curve $n(t)$, where j denotes the index for the order value p_j within $[p_{\min}, p_{\max}]$ and j increases as p_j increases; the order difference between the adjacent order components $\Delta p_j|_{j\geq 1} = p_j - p_{j-1}$,

(iii) $i = 0$, $f_i = f_{\min}$,

(iv) find the abscissa t_j of the intersection of the two curves: $f(t) = f_i$ and $f(t) = f_j(t)$, $j = 1, 2, \ldots, J$,

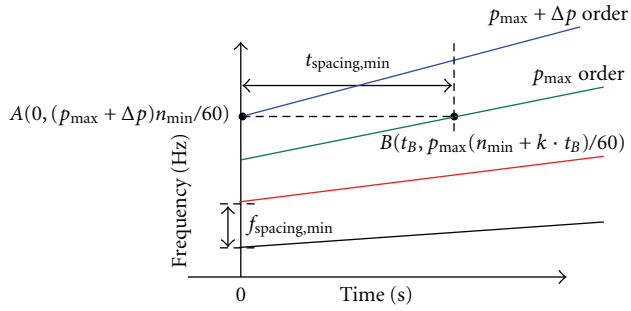

Rotary speed: $n = n_{min} + k \cdot t$
$n_{min}(r/min)$: the lowest rotary speed
p_{max}: the highest order of interest in a signal
Δp: the order difference between adjacent order components
$k(r/(min \cdot s))$: the change rate of the rotary speed

FIGURE 4: Schematic diagram for the theoretical time-frequency locations of order components in a signal with linearly increasing speed.

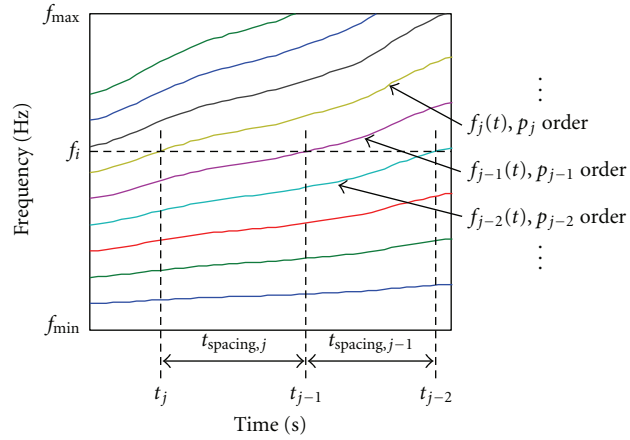

FIGURE 5: Schematic diagram for searching for $t_{spacing,min}$.

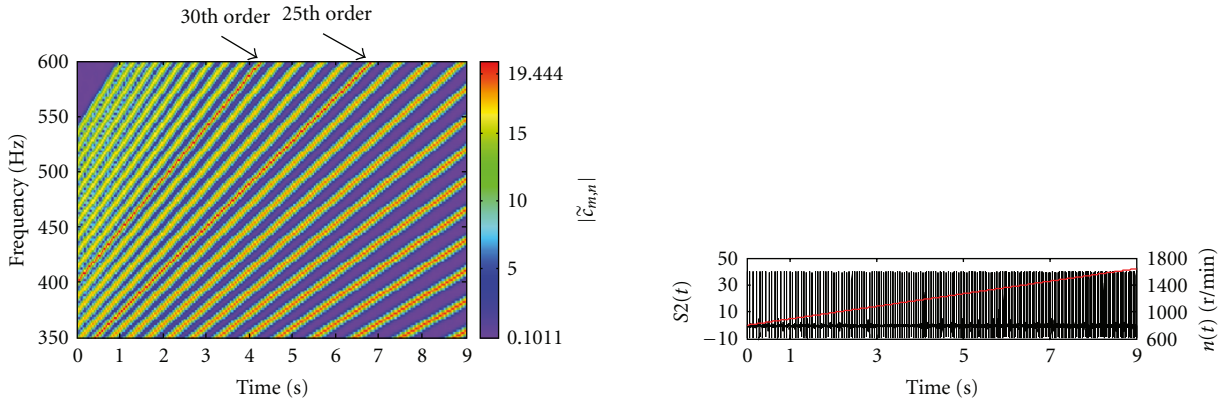

$\sigma_t = 40$ ms
$6\sigma_t = 240$ ms
$6\sigma_f = 11.93$ Hz
$\sigma_N = 0.08$
$f_s = 8192$ Hz
$L = 4096$
$\Delta M = 256$

(a) (b)

FIGURE 6: The Gabor coefficient spectrum of the simulation signal $S2(t)$ based on the improved flowchart. (a) Gabor coefficient spectrum of signal $S2(t)$; and (b) signal $S2(t)$ (in black) and the simultaneous speed $n(t)$ (in red).

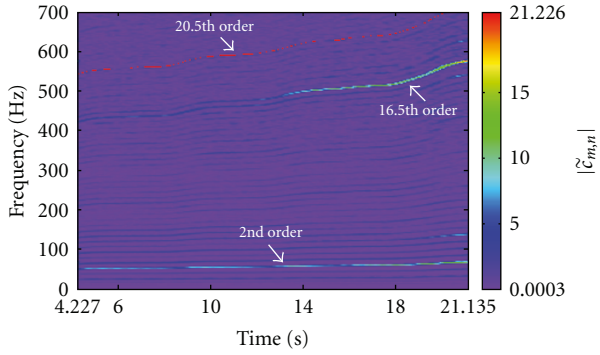

$\sigma_t = 80$ ms
$6\sigma_t = 480$ ms
$6\sigma_f = 5.968$ Hz
$\sigma_N = 0.08$
$f_s = 2048$ Hz
$L = 2048$
$\Delta M = 128$

(a)

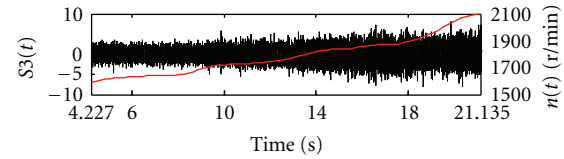

(b)

Figure 7: The Gabor coefficient spectrum of an actual signal $S3(t)$ based on the improved flowchart. (a) Gabor coefficient spectrum of signal $S3(t)$; and (b) signal $S3(t)$ (in black) and the simultaneous speed $n(t)$ (in red).

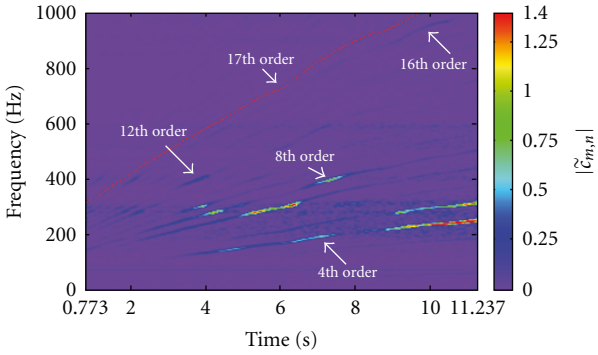

$\sigma_t = 37$ ms
$6\sigma_t = 222$ ms
$6\sigma_f = 12.9$ Hz
$\sigma_N = 0.0723$
$f_s = 4$ kHz
$L = 2048$
$\Delta M = 128$

(a)

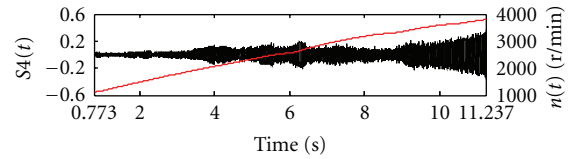

(b)

Figure 8: The Gabor coefficient spectrum of an actual signal $S4(t)$ based on the improved flowchart. (a) Gabor coefficient spectrum of signal $S4(t)$; and (b) signal $S4(t)$ (in black) and the simultaneous speed $n(t)$ (in red).

(v)

$$t_{\text{spacing},j} = \begin{cases} \left| t_j - t_{j-1} \right| & \left(\text{if both } t_j \text{ and } t_{j-1} \text{ exist}\right), \\ \infty & \left(\text{if neither } t_j \text{ nor } t_{j-1} \text{ exists}\right), \end{cases} \quad j = 1, 2, \ldots, J, \tag{16}$$

(vi) find the minimum of the set $\{t_{\text{spacing},j}\}_{j\geq 1}$ and assign it to $t_{\text{spacing},i}$,

(vii) $i = i + 1$, $f_i = f_i + \delta f$,

(viii) repeat steps (4)–(7) until f_i is larger than or equal to $f_{\max}$,

(ix) find the minimum of the set $\{t_{\text{spacing},i}\}$ and assign it to $t_{\text{spacing,min}}$.

5. Verification

To verify the effectiveness of the improved flowchart, a simulation signal is defined as

$$\begin{aligned} S2(t) &= \sum_{p=1}^{40} S_p + \text{Noise}|_{\text{SNR}=50(34\,\text{dB})} \\ &= \sum_{p=1}^{40} A_p \cos\left(\frac{2\pi p}{60}\left(n_{\min} t + \frac{k}{2} t^2\right)\right) \\ &\quad + \text{Noise}|_{\text{SNR}=50(34\,\text{dB})}, \end{aligned} \tag{17}$$

where $n_{\min} = 800\,\text{r/min}$, $k = 93.3\,\text{r/(min}\times\text{s)}$; the instantaneous amplitude of the p_{th} order component is:

$$A_p = 1. \tag{18}$$

For this signal, if the order range of interest is [1, 30] and the speed range of interest is above 800 r/min, then $f_{\text{spaing,min}}$ and $t_{\text{spacing,min}}$ determined with (13) and (14) are 13.3 Hz and 285.6 ms, respectively. Consequently the appropriate range for σ_t is [35.8, 47.6] ms. Figure 6 shows the result when σ_t equals to 40 ms. There are no overlaps between the order components with an order not larger than 30 in Figure 6(a).

We tested some real-world signals with simultaneous speeds not linearly varying. Figures 7 and 8 are two such examples. In both cases, a photoelectric tachometer was used to detect the simultaneous speed.

For signal $S3(t)$ (Figure 7), the order difference between the adjacent order components is 0.5, the ranges of interest are order range: [0.5, 20], speed range: [1,600, 2,100] r/min; frequency range: [0, 700] Hz. Then $f_{\text{spaing,min}}$ with (13) is 13.3 Hz and $t_{\text{spacing,min}}$ determined by numerical algorithm is 511.745 ms, which is between order 20.5 and order 20 at the 674 Hz frequency. Consequently, the determined range for σ_t with (11) and (12) is [35.8, 85.3] ms. Figure 7 shows the result when σ_t equals 80 ms. All order components with an order not larger than 20 are separated in Figure 7(a).

For signal $S4(t)$ (Figure 8), the order difference between the adjacent order components is 1, the ranges of interest are order range: [1, 16], speed range: [1,120, 3,800] r/min, and frequency range: [0, 1,000] Hz. Then $f_{\text{spaing,min}}$ with (13) is 18.7 Hz and $t_{\text{spacing,min}}$ determined by numerical algorithm is 219.382 ms, which is between orders 17 and 16 at the 340 Hz frequency. Consequently, the determined range for σ_t with (11) and (12) is [25.6, 36.6] ms. Figure 8 shows the result when σ_t equals 36 ms. All order components with an order not larger than 16 are well separated in Figure 8(a).

Our tests on simulation and real-world signals indicate that the proposed search of parameters for GOT is successful.

6. Conclusion

In this study, we designed an automatic search method to find appropriate analysis parameters for GOT, which eliminates the trial-and-error process. We first generalized the conditions for the minimum time spacing limit and the minimum frequency spacing limit from simulations, under which the Gabor coefficient spectrum with Gaussian window will well separate order components. The conditions were then utilized to generate an analysis window in the improved GOT flowchart. Our simulation results and real applications both verified its effectiveness. According to the improved flowchart, as long as $\sigma_{t,\min} \le \sigma_{t,\max}$, any value within $[\sigma_{t,\min}, \sigma_{t,\max}]$ for σ_t will guarantee well-separated order components in the Gabor coefficient spectrum. This is an important convergence condition for the reconstructed order waveform. The prerequisite for this improved GOT is with a proper speed-time curve and prior knowledge on order differences between adjacent order components. Usually, the simultaneous speed-time curve is easy to acquire by a tachometer, and Δp_j can come from prior knowledge about the test objects or be determined by preliminary trials. For the GOT of signals without simultaneous speed information, automatic search of appropriate processing parameters should deserve future research.

References

[1] S. Gade, H. Herlufsen, H. Konstantin-Hansen et al., "Order tracking analysis," Technical Review 2, Brüel & Kjær, 1995.

[2] S. Gade, H. Herlufsen, H. Konstantin-Hansen et al., "Characteristics of the Vold-Kalman order tracking filter," Technical Review 1, Brüel & Kjær, 1999.

[3] M. C. Pan and C. X. Wu, "Adaptive Vold-Kalman filtering order tracking," *Mechanical Systems and Signal Processing*, vol. 21, no. 8, pp. 2957–2969, 2007.

[4] S. Qian, "Gabor expansion for order tracking," *Sound and Vibration*, vol. 37, no. 6, pp. 18–22, 2003.

[5] M. C. Pan, S. W. Liao, and C. C. Chiu, "Improvement on Gabor order tracking and objective comparison with Vold-Kalman filtering order tracking," *Mechanical Systems and Signal Processing*, vol. 21, no. 2, pp. 653–667, 2007.

[6] H. Shao, W. Jin, and S. Qian, "Order tracking by discrete Gabor expansion," *IEEE Transactions on Instrumentation and Measurement*, vol. 52, no. 3, pp. 754–761, 2003.

[7] S. Qian, *Introduction to Time-Frequency and Wavelet Transforms*, Prentice Hall, Upper Saddle River, NJ, USA, 2002.

[8] S. Qian and D. Chen, "Optimal biorthogonal analysis window function for discrete Gabor transform," *IEEE Transactions on Signal Processing*, vol. 42, no. 3, pp. 694–697, 1994.